Journal of Engineering Research and Reports

20(12): 64-90, 2021; Article no.JERR.72533
ISSN: 2582-2926

Evaluation of Spatio-Temporal Soil Moisture Variability in Semi-Arid Rangeland Ecosystem, Maasai Mara National Reserve, Kenya

Charles C. Kapkwang[1,2*], Japheth O. Onyando[2], Peter M. Kundu[2] and Joost Hoedjes[3]

[1]Department of Agricultural Biosystems and Economics, University of Kabianga, P.O. Box 2030 - 20200, Kericho, Kenya.
[2]Department of Agricultural Engineering, Egerton University, P.O. Box 536 - 20115, Egerton, Kenya.
[3]Department of Water Resource and Earth Observation Science, University of Twente, Netherlands.

Authors' contributions

This work was carried out in collaboration among all authors. All authors read and approved the final manuscript.

Article Information

DOI: 10.9734/JERR/2021/v20i1217421
Editor(s):
(1) Dr. Heba Abdallah Mohamed Abdallah, National Research Centre, Egypt.
Reviewers:
(1) Nooshin Sajjadi, Islamic Azad University, Iran.
(2) Lupupa Kachenga, Eden University, Zambia.
Complete Peer review History: https://www.sdiarticle4.com/review-history/72533

Original Research Article

Received 16 June 2021
Accepted 23 August 2021
Published 02 September 2021

ABSTRACT

Aim: To evaluate the spatio-temporal soil moisture storage and retention capacities in semi-arid rangeland ecosystem, Maasai Mara National Reserve (MMNR), Kenya
Study Design: Randomized complete block design (RCBD) of reference Cosmic Ray Neutron Sensor (CRNS) station, ten-(10) spatially distributed (soil moisture and temperature capacitance) probes (5TM-ECH$_2$0) sites.
Place and Duration of Study: Kenya, MMNR, the oldest natural semi-arid rangeland ecosystem and globally unique for the great wildebeest migration, between May 2017 and April 2019.
Methodology: Soil moisture (SM) variation data was collected using (CRNS) at spatial and point-scale 5TM-ECH$_2$O probes, and gravimetric water content from (10) spatially distributed stations. Both CRNS and 5TM-ECH$_2$O probes were used to monitor near-real time moisture levels at different soil layers ranging between 0-5cm, 5-10cm, 15-20cm, 35-40cm, and 75-80cm. Soil physical and chemical properties were laboratory analyzed. Calibration and validation datasets

**Corresponding author: Email: ckewel2010@gmail.com, ckapkwang@kabianga.ac.ke;*

were obtained from 5TM-ECH$_2$O probe and gravimetric soil samples extracted from respective layers and sites.

Results: The pedological characteristics of the investigated ecosystem soil profile indicate decreased bulk density by 2.1% to 11.12% from upper layers (0-5cm) to deeper layers at (75–80 cm). Across the rangeland, 70% of soil textural classes were sandy clay loam (SCL) with higher clay percent and 30% sandy clay (SC) and soil porosity varied between 30.1% and 51% in the ecosystem. Moreover, volumetric water content (VWC) of spatially distributed 5TM-ECH$_2$O probes ranged between 0.11m^{3}m^{-3} and 0.32m^{3}m^{-3} during wet season with mean VWC of 0.16m^{3}m^{-3}, however, the VWC ranged between 0.04 m^{3}m^{-3} and 0.17m^{3}m^{-3} during the dry season with a mean volume of 0.11m^{3}m^{-3} across the rangeland ecosystem.

Conclusion: In this study, SM exhibited an annual periodicity of seasonal variation of spatial and temporal moisture partitioned as moisture gaining, losing, and a moisture stable period. This probably could be a consequence of increased movement of water to deeper layers caused by high precipitation and less evaporative demand caused by lower temperatures. The calibrated CRNS probe provided good estimates of spatial soil moisture variation when calibrated with 5TM-ECH$_2$0 and gravimetric sampling in relation to precipitation events and that deeper soil layers showed higher amount of soil moisture than shallow layers. The findings of the study will provide better formulation of the ecosystem vegetation management policies, conservation and planning for sustainable wildlife tourism industry.

Keywords: Soil moisture; variability; storage; capacities; rangeland; ecosystem.

1. INTRODUCTION

Soil moisture (SM) is a fractional state variable of hydrological process that occurs due to the partitioning of precipitation into infiltration and runoff, also influenced by energy fluxes such as latent and sensible heat acting at the atmosphere and near the land surface. Rainfall-runoff processes majorly control the availability of soil moisture and this occurs due to the distribution of soil moisture that varies tremendously over time and space. MMNR has over decades experienced the effect of land degradation caused by encroachment of riparian community coupled with climate variability and as a result this influence the bi-seasonal (dry and wet) vegetation change deteriorating biomass quality and quantity for wildlife/livestock forage production. This study was undertaken to evaluate the influence of climate variability on soil moisture regimes in semi-arid rangeland ecosystem. This in relation to vegetation dynamics is important for sustainable feedstock to wildlife/livestock reliance as a means of economic hub and livelihood development through tourism industry. Nonetheless, there has been undetermined spatio-temporal variation of soil moisture and scarce climatic data in semi-arid MMNR rangeland to provide adequate information of the ecosystem's behavior yet because of zebras and massive annual wildebeest migration. However, there is an inherent difficulty of remotely sensed soil moisture measurement in relating soil moisture variability at the scale of the footprint to larger or smaller scale [1]. The soil water balance is a valuable tool for analyzing the impacts of land-use changes on soil water storage and to designing adaptation strategies for global change scenarios as far as water resources management is concerned [2]. The authors ([3] [4] utilized distributed sensor networks to examine the cosmic-ray sensing (CRS) soil moisture method at the small watershed scale in two semiarid ecosystems of the southwestern United States of America. They author found spatial variability of soil moisture is linked to the spatially averaged conditions through predictable relations that do not vary significantly across the study sites. For higher mean soil moisture, they observed a near linear increase in spatial variability followed by an asymptotic behavior attributed to the seasonally wet conditions during the North American monsoon. The author [5] in a study of semi-arid ecosystem pinpointed out that combining fixed and mobile CRS method can establish landscape scale (102 to 103 km^2) soil moisture monitoring networks at grid sizes (~1km^2) comparable to land surface modeling. According to [6], the soil water storage is the total amount of water stored in the soil within the plant's root zone. A deeper rooting depth means there is a larger volume of water stored in the soil and therefore a larger reservoir of water for the crop to draw upon between rainfalls. Stored water in soil is a dynamic property that changes spatially in response to climate, soil properties, topography, and temporally because of

differences between utilization and redistribution via subsurface flow [7]. The soil water content is the amount of water held in the soil at any given time and can be expressed as volumetric or gravimetric water content. The flow of water through soil is controlled by the size and shape of pores, which in turn is controlled by the size and packing of soil particles. For many purposes, the particle size distribution is characterized by the soil texture, which is determined by the proportions by weight of clay, silt, and sand. [8] analyzed soil moisture variability under various climatic conditions while other extrinsic factors such as soil texture, vegetation, land management, and topographic conditions) were more or less similar. Once gravitational soil moisture drainage has ceased, changes in soil moisture storage due to transpiration will no longer affect the relationship between base-flow and storage [9]. The effects of temperature on plant growth are largely mediated by its effects on chemical reactions (e.g., photosynthesis and respiration) and its effects on soil moisture [10]. [11] in a modeling study found varying soil moisture changes in different regions with a predominant pattern of decreased soil moisture with increased temperatures.

2. MATERIALS AND METHODS

2.1 Description of the Study Area

The Maasai Mara rangeland and ecosystem (Figure 1) lies in southwest of Kenya (1^0 29`35``N and $035^o$ 08` 57``W) and is approximately 1,530 square kilometres, of which less than 10% represents MMNR, while the rest is the unprotected land inhabited by the agro-pastoral community and conservancies. The area lies at an altitude of about 1,600 m above sea level, the Maasai Mara rangeland ecosystem is an area of undulating savanna/woodland intersected by numerous drainage lines and bisected by the Mara River [12]. The temperature range is 12 to 28^0C and annual rainfall normally lies within the range of 800 – 1,200 mm, with a northwest to southeast declining gradient. Rainfall is bimodal, with a main dry period from mid-June to mid-October and a shorter dry season during January and February.

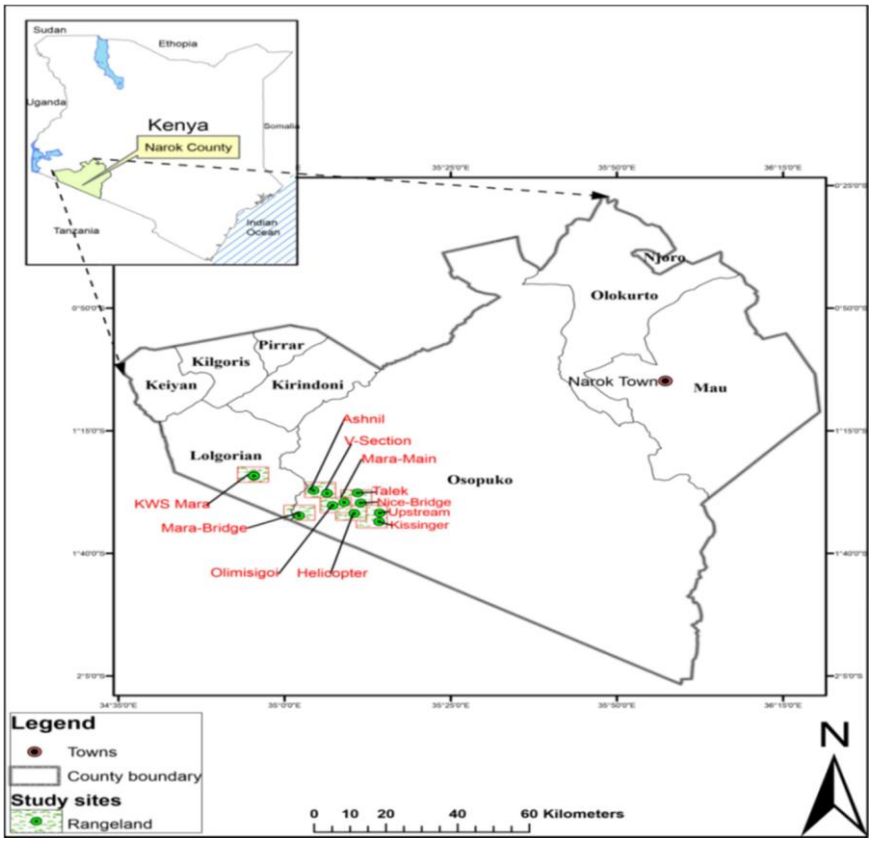

Fig. 1. Map of Maasai Mara Rangeland Ecosystem

2.2 Soil Physical and Chemical Properties of Maasai Mara Rangeland Ecosystems

2.2.1 Soil Texture

Soil texture for 24 selected sampling points at bearing angles of (0, 60, 120, 180, 240 and 300) degrees and radii distance of (10, 25, 75 and 175) m in the study area denoted as A, B, C and D rings were collected, labelled and taken for laboratory analysis. For each field test, 96 soil samples were collected from 24 sampling points at depths of midpoint range 0-5cm, 5-10cm, 10-15cm, 15-20cm, 20-25cm, and 25-30cm for biophysical soil properties characterization, which included texture, bulk density, particle density, and the intended ecosystem soil moisture variation. Laboratory analysis of physical and chemical properties was determined at Kenya Agricultural and Livestock Research Organization (KALRO), National Agricultural Research Laboratories, Kabete, Kenya (NARL). Textural classes were determined using the standard procedure of sieving and sedimentation analysis based on Stokes' Law (hydrometer method) [13], where soil were dispersed using (sodium hexameta phosphate), and mixed with water (soil suspension). The settling velocity of individual particles were determined depending on particle diameter and forces acting on soil particle as gravitation, buoyancy and drag forces, and all depended on particle size. Stokes' law written as equation (2.1) gave the free fall velocity;

$$v = \frac{1}{18}\left(\frac{(\rho_s - \rho_F)gd^2}{\mu}\right) \quad (2.1)$$

where, v = settling velocity, g = gravitational acceleration, g = 9.80ms^{-2} ρ_s = density of dropped object d = diameter of dropped object, ρ_F = density of fluid, μ = viscosity of fluid. Soil mixture was finally classified according to soil textural triangle, where determined percentage distributions of sand, silt and clay particles were characterized to give the soil's textural classes [14].

2.2.2 Bulk Density

Bulk densities for each soil depths were also determined by gravimetric coring method used by [15, 16]; and a water pycnometer was employed to find the soil particle density, ρ_z. .

2.2.3 Soil Organic Matter

The Organic Carbon (% OC) was analyzed by Walkey and Black procedure [17]. Organic matter (OM %) was calculated by multiplying OC with conventional Vanbameller factor. The values of organic carbon were multiplied by a Vanbameller factor of (58%) 1.724 to obtain values for organic matter content available in the soil. The organic matter content was measured as the Cox in %. These values were converted into the organic matter in percentage using the conversion equation OM = 1.724 Cox (%).

2.4 Cosmic-Ray Probe Soil Moisture Measurements

Continuous spatial monitoring of soil moisture at 0-5cm, 5-10cm, 15-20cm, 35-40cm and 75-80 cm depths at the study site were performed using a cosmic ray soil sensors (Model CRS-1000 from Hydroinnova LLC, Albuquerque, NM, USA) and (5TM, Decagon Devices, Inc.) connected to a data logger. During the seasonal field visits, undisturbed soil samples were collected within CRNS site and 5TM-ECH2O stations at specific profile depths of 0-5cm, 5-10cm, 10-15cm, 15-20cm, 20-25cm, and 25-30cm, 35-40cm and 75-80cm represented by 2.5cm, 7.5cm, 12.5cm, 17.5cm, 22.5cm and 27.5cm, 37.5cm and 77.5cm.

Spatially distributed sampling points footprint were in distances of 10m, 25m, 75m, and 175m from the CRNS center using core-sampling rings (5cm diameter, 5cm height) which allowed further soil measurements properties under controlled laboratory conditions. The soil water content was determined according to the described method as follows;

2.4.1 N_o - method

The author [23] developed a shape-defining function, hereafter called N_o - method, to determine volumetric soil water content θ_{vol} (cm^{3}cm^{-3}) directly from corrected neutron flux:

$$\theta_{vol} = (a_0 + \rho_{bd}) \times \left(\frac{N_{pih}}{N_0 - a_1}\right)^{-1} - (a_2 - \rho_{bd}) \quad (2.3)$$

where, the parameters a_0 = 0.0808, a_1 = 0.372, a_2 = 0.115 are dimensionless and N_o is a site-specific calibration parameter. It was assumed that the parameters a_0 , a_1 and a_2 are constant in time and independent of soil chemical composition [24, 25]. The N_o is a time-constant site-specific calibration parameter that depends mainly on the site-specific environment and reference conditions.

2.4.2 Field calibration and validation of cosmic ray soil moisture sensor

During the field study, there were 10 calibration campaigns throughout the bi-seasonal period of the year in 2017 to 2019. The initial occurrence was in the month of February during the rainy season when the conditions were very wet soils. For all the calibration campaigns, the recommended sampling pattern for the calibration of CRNS were followed, which was developed by [26] was slightly modified as detailed in [27]. The sampling pattern prescribed four concentric circles around the CRNS with radii of 10, 25, 75, and 175m (Figure 3). The four circles were intersected uniformly by six straight lines that point from the sensor towards the subsequent bearings north (0°), northeast (60°), southeast (120°), south (180°), south- west (240°) and north-west (300°). The samples were taken at nearly all intersections, which were at exact pegged spot of intersection. The sampling pattern followed guaranteed each sample an equal weight towards the spatial mean of soil moisture that was detected by CRNS, considering sensitivity of the CRNS decreased exponentially with distance. Core ring samplers were used to extract 30 cm soil cores at 18 locations within the footprint of the sensor afterwards dividing each soil core into six 5 cm thick soil samples 0-5cm (0.25cm), 5-10cm (7.5cm), 10-15cm (12.5cm), 15-20cm (17.5cm), 20-25cm (22.5cm) and 25-30cm (27.5cm). For each of the 10 calibrations this left us with 108 soil samples, which were carried in sealed plastic bags placed in a cooler box where the samples were taken for analysis at Maasai Mara University chemistry laboratory to determination of gravimetric water content (GWC). The samples were immediately weighed, oven-dried at 105°C for 24 h, and then weighed again to determine their volumetric water content and their bulk density. Afterwards soil texture, particle density, total organic carbon, and root biomass were determined for five depth-representative soil samples at KALRO and NARL. To this end, the 108 samples (taken from the last calibration campaign in November) were grouped by sampling depth. From each of the 18 samples per sampling depth, 2g were extracted, mixed to create a single bulk sample per depth range 0-5cm, 5-10cm, 15-20cm, 35-40cm, and 75-80cm. After that, the lattice water was also removed from the samples and was sent for analysis in Australian Laboratories. In the determination of soil organic matter (SOM), the already oven-dried samples were then weighed, and placed in the oven for another 24 h at a temperature of 400°C. This was done following procedure by [28], [29], through “loss on ignition” procedure since the organic matter is burned off in the process. Here, the soil organic matter and root biomass is removed from the samples. After weighing the samples, the fractional computation of combined soil organic matter and root biomass was done by placing samples again in the oven for 24 h, this time at a temperature of about 1000°C. In order to make soil organic matter and root biomass comparable to the influence of pure water, this was then converted into equivalents of water by multiplying their weight by 0.556, which is the ratio of 5 times the molecular weight of water. Here, the molecular weight of cellulose was taken into account that cellulose ($C_6H_{10}O_5$) contains 10 hydrogen atoms per molecule while water (H_2O) only contains 2) following the method of [28] [30]. The neutron counts from the sensor were smoothed with a 12 h moving window to reduce measurement noise [31]. The step followed was to correct the neutron counts for variations in (a) pressure, (b) incoming neutron flux and (c) water vapor in the air using equation (2.5) of [24].

2.4.3 Calibration of cosmic ray soil moisture sensor by gravimetric sampling

For calibration campaigns, the recommended gravimetric soil-sampling pattern for the calibration of CRS developed by [26] was followed and slightly modified as detailed in [27]. For each of the 24 calibrations points, 144 soil samples were extracted using a core ring (5cm diameter, 5cm height) from profile depths of 0-5cm, 10-15cm, 15-20cm, 35-40cm intervals down to 75-80cm from the concentric sampling (coordinate) points at four radial rings at 60, 120, 180, 240, 300 and (0, 360) degrees.

Fig. 2. Installed cosmic-ray soil moisture neutron sensor probe

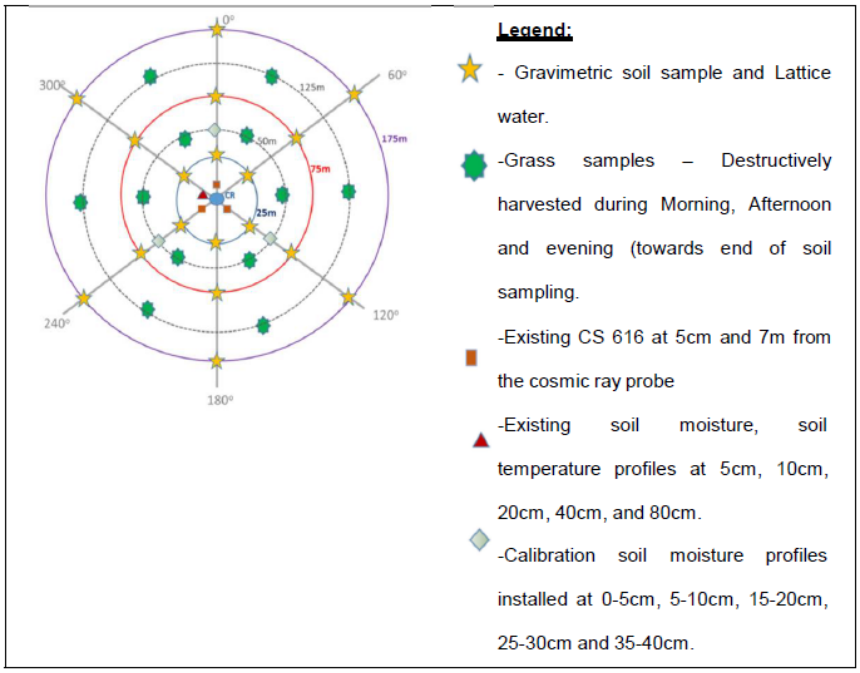

Fig. 3. Calibration procedure for gravimetric soil sampling

Fig. 3 indicate the steps followed in calibration where pits/trenches of 50cm by 100cm were dung to a depth of 100cm to allow possible core sampling to the bottom depth of the pit. Soil samples were taken on 20th May 2018 to calibrate N_o and determine site-specific parameters. The excavated soil samples were filled in plastic bags and transported to the laboratory within less than 10 hours. These wet field soil samples were weighed, placed into a ventilated oven, and dried at 105°C for 48 hours. The samples were finally weighed, then reweighed to constant final weights. Based on mass balance, the gravimetric water content was converted to volumetric water content by multiplying with the bulk density. In the calibration of CRNS, a representative bulk density value is required to convert the gravimetric soil moisture content to volumetric water content. However, CRNS measures the volumetric soil moisture content, which is expressed as the ratio of volume of water to the total volume of the soil sample (m^3m^{-3}). The bulk density determination was obtained via extraction of undisturbed soil core rings at various locations and depths within the rangeland.

Here, the calibration target was to determine the average N_0 value (site-specific calibration parameter), which is the theoretical neutron intensity (counting rate) in air above dry soil (no moisture).

The data from the CRNS are sent mainly in

hourly basis, via satellite link. The calibration procedure followed that of [7, 31]. The initial calibration procedure was to correct the neutron counts. This correction involved determining the neutron correction factors, using the following equations.

$$N_{corr} = \frac{N^{'} \times CP \times CWV}{CI \times CS} \quad (2.4)$$

where, N_{corr} is the corrected neutron counts per hour, N' is the raw moderated neutron counts, CP is the pressure correction factor, CWV is the water vapour correction factor, CI is the high-energy intensity correction factor, and CS is the scaling factor for geomagnetic latitude.

$$CP = \exp\left(\frac{P_O - P}{L}\right) \quad (2.5)$$

where, L is the mass attenuation length for high-energy neutrons (gcm^{-2}), P is the atmospheric pressure (mb) at a specific site and P_0 is the reference atmospheric pressure (mb).

$$CWV = 1 + 0.0054(P_{vo} - P_{vo}^{\ ref} \quad (2.6)$$

where, P_{vo} is the absolute humidity of air (gm^{-3}) and P_{vo} ref is the reference absolute humidity of the air (gm^{-3}).

$$CI = \frac{I_m}{I_{ref}} \quad (2.7)$$

where, *lm* is the selected neutron monitoring count rate at any particular point in time and Iref is the reference count rate for the same neutron monitor from an arbitrary fixed point in time. The neutron flux data was obtained through the neutron-monitoring database (www.nmdb.eu), which provides real-time data from a global network of monitoring stations.

$$CI = f(x, y, z, t) \quad (2.8)$$

where, x, y, z is location and elevation, and t is time. The following calibration function was then used to determine the No value for each calibration.

$$\left(\theta_p + \theta_{lw} + \theta_{soc}\right) = \frac{0.0808}{N/N_o - 0.372} - 0.115 \quad (2.9)$$

Rearranging the calibration function to determine,

$$N_0 = \left(\frac{N}{\frac{0.0808}{\left(\theta_p + \theta_{lw} + \theta_{soc}\right)\rho_{bd} + 0.115} + 0.372} \right) \quad (2.10)$$

where, θ_p is the gravimetric water content (gg^{-1}), θ_{lw} is lattice water content (gg^{-1}), θ_{soc} is soil organic carbon water content (gg^{-1}), ρ_{bd} is dry soil bulk density (gcm^{-3}), N is the corrected neutron counts per hour, and N_0 is an instrument-specific calibrated parameter.

$$VWC = \left(\frac{0.0808}{\left(\frac{N}{N_o}\right) - 0.372} - 0.115 - \left(\theta_p + \theta_{lw} + \theta_{soc}\right)\rho_{bd} \right) \quad (2.11)$$

Notably, here soil moisture is often expressed in units of volume percent,

$$VWC(\%) = \theta_p \times \rho_{bd} \times \theta_{soc} \times 100$$

θ_{soc} was not determined, but was given a value of 0.01 gg^{-1} based on published values. θ_{lw} was determined to be 0.154 gg^{-1}. This was a 50-g representative soil sample sent to Activation Laboratories in Canada for θ_{lw} determination by combustion at 1000°C. Correction for biomass was also computed using equation.

$$\left(\theta_p + \theta_{lw} + \theta_{soc}\right) = \frac{0.0808}{\frac{N}{N_o(BWE)} - 0.372} - 0.115 \quad (2.12)$$

where, BWE is the biomass water equivalent

(mm). The biomass calculation is usually done for vegetation types whose biomass changes with their growing stage, but because vegetation in MMNR were dominant short grasslands of different species, the biomass was negligibly small hence change in biomass was therefore insignificant, and a biomass correction was not required. In each calibration, the neutron count (N) was determined as the average neutron count during which the calibration soil samples were obtained. These counts were used to determine the N_0 value for each calibration as indicated using the rearranged calibration equation (2.9).

2.4.4 Calibration by SMST Capacitance Probes

In the study, 10 (ten) 5TM-ECH$_2$O (soil moisture, soil temperature campaign sensor) stations were installed at various spatially distributed points in MMNR ecosystem for moisture monitoring. The 5TM-ECH$_2$O sensor probes at each point were horizontally placed in soil profiles as follows; first layer was ranged between 0 - 5cm, second layer between 5-10cm, third layer at mid-point of 15 - 20cm, fourth layer between 35 – 40cm and the fifth layer was finally ranged at mid of 75cm – 80cm.

Five combined 5TM-ECH$_2$O probes labeled **P1** (0-5cm), **P2** (5-10cm), **P3** (15-20cm), **P4** (35-40cm) and **P5** (75-80cm) were inserted below the soil segments to continuously measure soil water content at temporal resolution of 15mins interval. A laboratory calibration database on gravimetric water content, 5TM-ECH$_2$O probes were used to determine and statistically verify the accuracy of the CRNS. Ten spatially distributed stations of 5TM-ECH$_2$0 probes with their co-ordinates recorded via Garmin GPS60 were located as shown in (figure 5). The direct measurement of VWC as soil moisture was simultaneously measured from respective segment and recorded via (CS616, Campbell Scientific Inc., UK) data-logger. The data was downloaded via USB to the remote computer for further analysis. In this study, from 108 samples of shallow depth SMC data collected, the depth-averaged SMC of each site at each measuring time was calculated using equation (2.13):

$$SMC_j = \frac{1}{n}\sum_{n=1}^{n} SMC_n \tag{2.13}$$

where, n is the number of measurement layers at the site j, and SMCn is the mean soil moisture content in layer n calculated by five sampling profiles. The temporal-averaged shallow SMC of each site was also calculated by using equation (2.14):

$$SMC_n = -\sum_{n=1}^{n} SMC_j \tag{2.14}$$

where, n is the number of measurement times at the site j.

Samples were also measured for bulk density (dB), soil textural classification, particle density, total organic matter (TOC), surface hydraulic conductivity (infiltration rate) and soil chemistry (pH) at incremental depths to 80cm. The gravimetric soil moisture content is usually expressed by weight as the ratio of the mass of water present to the dry weight of the soil sample (g/g). The temporal resolutions for the 5TM-ECH$_2$O sensor probes manufactured by Decagon Devices Corporation, USA measurements were at 15 mins time-series, where the sensors signals were captured and recorded via Decagon data loggers. The soil moisture data were weighted averaged for each station on daily time-step to enable easy handling.

2.4.5 Gravimetric water content

The VWC was determined via gravimetric method from soil samples collected at the spatially distributed stations and around the main weather station where cosmic ray neutron sensor and 5TM-ECH$_2$0 probes were installed. In this analysis, 144 soil samples were spatially collected during field visits using sampling core rings measuring (5cm diameter, 5cm height) and were kept in a cooler box, was then oven dried in a constant temperature room of 105^{o}C for 24 hours.

2.5 Statistical Analysis

In the study, analysis of variance (ANOVA) were performed using the PROC GLM procedure in SAS to determine significant effects of bulk density, particle density, total porosity, total organic carbon and soil organic matter to soil moisture scenarios. Fisher's protected least significant difference (LSD) was used to separate treatment means. Regression analysis was performed using the SAS PROC REG procedure

Fig. 4. Installed 5TM-ECH$_2$O Soil Moisture and Temperature Capacitance probes

in SAS [32]. The soil moisture content from different stations was described statistically using their (mean, variance, maximum, and minimum value, standard deviation and coefficient of variation (Table 3.10). The relative mean difference δ_{ij} was calculated and presented graphically in order to show the rank of wettest, driest and mean points in the area for each year (figure 8, 9 and 10). This technique ranks the measurement locations based on the relative difference from the spatial mean [32]. The relative mean difference was calculated as follows;

$$\delta_{ij} = \frac{\Delta_{ij}}{S_j} \tag{2.15}$$

where, Δ_{ij} is calculated by the difference between the measurements at each point (i) on day (j) and the mean measurement for day (j), and $S\ j$ represents the field mean soil water storage for a particular day (j). For each location, the average and standard deviation of δ_{ij} , were calculated, tabulated and graphically presented.

3. RESULTS AND DISCUSSION

This section shows the results of soil samples excavated from CRNS concentric periphery and ten 5TM-ECH$_2$0 probe stations for laboratory analysis to determine; their soil texture, total organic carbon (TOC), soil organic matter (SOM), particle density, bulk density, and total porosity, which were subsequently used to calculate gravimetric water content. Spatially determined soil properties and volumetric water content from different 5TM-ECH$_2$0 sites with varied profile depths were subsequently displayed in the tables and figures therein.

3.1 Soil Texture

Fig. 5 shows the sampling locations of ten 5TM-ECH$_2$O stations namely, Main Mara, V-section, Nice Bridge, Talek, Helicopter, Olimisigioi, Upstream, Kissinger, Ashnil and Mara Bridge. The determined soil type at Mara main station were sandy clay loam (SCL) within the top soil depth range of 0-10cm while below 10cm and between 10-80cm depth, the soil are sandy clay with mean particle size distribution of 71% sand, 22% clay and 7% silt and 55% sand, 39% clay and 7% silt respectively. On average across the rangeland segments, the particle size distribution shown that 70% of SCL and 30% of SC were spatially distributed. The mean particle fraction observed across the rangeland was distributed as 67% sand, 25.3% clay and 7.7% silt. Olimisigioi has varied soil type layers from top 0-10cm with sandy clay loam, clay soil at 20cm, sandy clay loam at 40cm while at 80cm the soils are sandy clay. The layers below from 20-80cm have variable soil types with mainly sandy clay except nice bridge with uniform sandy clay loam from top to bottom layer. The results of soil texture grade indicate that in this natural grassland vegetated ecosystem, the soil surface layers across the catchment are mainly sandy clay loam.

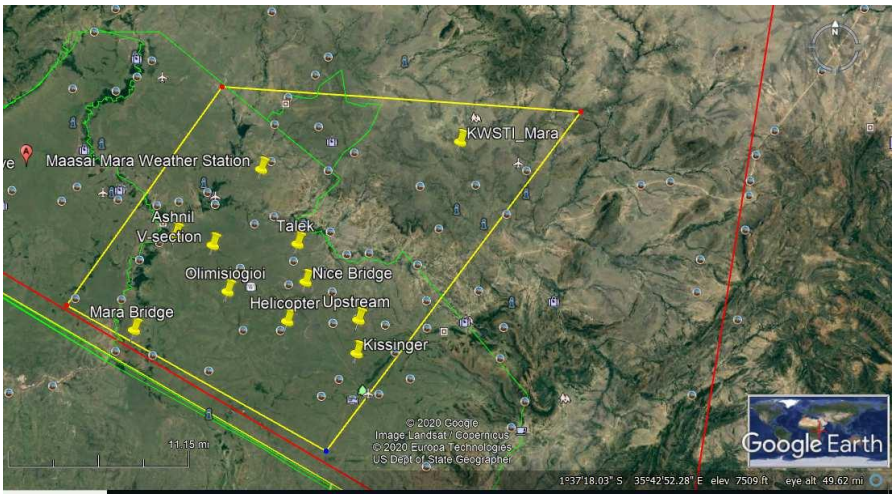

Fig. 5. Spatially distributed soil moisture, soil temperature, and soil sampling station sites

Table 1. Spatially distributed soil textural classes varied with depths across the Maasai Mara National Reserve rangeland ecosystem

S. No.	Station	Soil Depth (cm)	0-5	5-10	15-20	35-40	75-80
1.	Mara Main	Soil Texture	SCL	SCL	SC	SC	SC
2.	Kissinger	,,	SCL	SCL	SCL	SCL	SCL
3.	Ashnil	,,	SCL	SL	SCL	SCL	SCL
4.	Mara Bridge	,,	SCL	SL	SCL	SCL	SCL
5.	Helicopter	,,	SL	SL	SCL	SCL	SCL
6.	Olimisiogioi	,,	SCL	SCL	C	SCL	SC
7.	Talek	,,	SCL	SCL	SC	SC	SC
8.	Upstream	,,	SCL	SC	SC	SC	SC
9.	V-section	,,	SCL	SCL	SC	SC	SC
10.	Nice-Bridge	,,	SCL	SCL	SCL	SCL	SCL

Key: SC – Sandy Clay, SCL – Sandy Clay Loam, SL – Sandy Loam, C - Clay

Table 1 indicates a range of soil types existing in MMNR ecosystem, and that the textural classes were made of homogenous sandy clay loam (SCL) in most locations. The dominant segments occupies 62% (SCL) and rest 48% soils were distributed as 28% (SC), 8% (SL), 2% (C) and this appeared different as depth increased from the top soil surface layer to the bottom layer (5cm - 80cm) across the ecosystem. The soil type within the top 2.5cm layer at distance of 10m away from the center of the cosmic ray neutron sensor (CRNS) was sandy clay (SC) attributed to high organic content with the mean particles size distribution 76.6% sand, 16.3% clay and 7% silt. This was tested within 6 sample locations concentrically distributed at angles of 60 degrees as A60, A120, A180, A240, A300 and A360, 0. The classification were defined according to texture groups for unconsolidated parent material, as given by [33] based on USDA texture classes, as respectively coarse (S, LS, SL or approximately sand > 50% and clay < 20%), medium (L, SCL, CL, Si, SiL, SiCL) and fine (SC, SiC, C or approximately clay > 40%).

3.1.2 Bulk Density

Similar soil samples were then taken to the laboratory for determination of the compacted soil bulk density and the results were as follows; for soils at the Main Mara station and according to the soil depth, 0-5cm, 5-10cm, 15-20cm, 35-40cm and 75-80cm, the soil bulk density were 1.40g/cm^{-3},1.45g/cm^{-3}, 1.34g/cm^{-3}, 1.19g/cm^{-3} and 1.25gcm^{-3} respectively. This indicates that surface layer in this area have high bulk density as compared to the bottom layer density as it decreases gradually with depth. The bulk density of soil at Kissinger 5TM-ECH$_2$0 station shows that it oscillates between 1.72gcm^{-3} and 1.52g/cm^3 at 0-5cm and 75-80cm soil depth respectively. This indicates that soil density depends highly on soil mineral particles, which are aggregated depending on soil profiles. The

average measured bulk density obtained was 1.34gcm^{-3}. High bulk density value result from dense grass cover, high organic matter content, platy soil structure, high porosity, high sandy clay loam (SCL) soil layers and compaction caused by wildlife trampling; off-road tourist tracks and encroachment of Maasai herds.

The analysis of variance indicates no significant differences in mean bulk density across depths P1 (0-5cm) and P5 (75-80cm) in the entire rangeland ecosystem. P3 (15-20cm) was found to have a significantly higher bulk density of 1.34 gcm^{-3} than P2 and P4 with bulk densities of 1.29 gcm^{-3} and 1.27 gcm^{-3} respectively. At depth P5, (75–80 cm) the bulk density across the ecosystem significantly lower at 1.23gcm^{-3} as compared to P1 and P4 with 1.25gcm^{-3} and 1.27gcm^{-3} respectively. The significant differences in bulk density at P3 (35-40cm) are presumably due to compression of this depth resulting from increased elasticity of the soil due to its elevated moisture content at P1 and P2 as compared to P5, however there was no observed measurable compression.

3.3 Particle Density

With the same soil samples that were collected from five depths or layers at Mara Main station, Kissinger and Ashnil and across the other stations within the catchment, particle density were determined based on Bouyoucos Hydrometer method and described according to [13]. The average particle density of the soil at the Mara main station on profile depths of 0-5cm, 5-10cm, 15-20cm, 35-40cm and 75-80cm shows that the particle density were respectively 2.46 gcm^{-3}, 2.37 gcm^{-3}, 2.5 gcm^{-3}, 2.38 gcm^{-3} and 2.53 gcm^{-3}. The standard deviation of the particle density was 0.332 gcm^{-3}. The other soil moisture, temperature stations, that is Kissinger, Ashnil, Mara Bridge, Talek, Nice bridge, V-section, Olimisigioi and helicopter has almost constant average particle densities ranging from 2.40 g/cm^3 to 2.55gcm^{-3}.

Table 2. Statistical separation of means

Source	Sum of squares (SS)	Degrees of freedom (df)	Mean squares (MS)	P value	CI (%)	SD	F statistics	LSD
Between Groups	2.024	9	0.140	≤0.05	95	1.250	0.090	4.321
Within Groups	0.066	40	1.563					
Total		49						

P value - Significant at the 0.05 probability level, F – F ratio, CI – Confidence interval level (%), SD – Standard deviation, LSD, least significant difference between means. Mean Square of Profile (MSP) - 0.140, Mean Square Error (MSE) – 1.563, Sum of Square Error (SSE) – 0.695

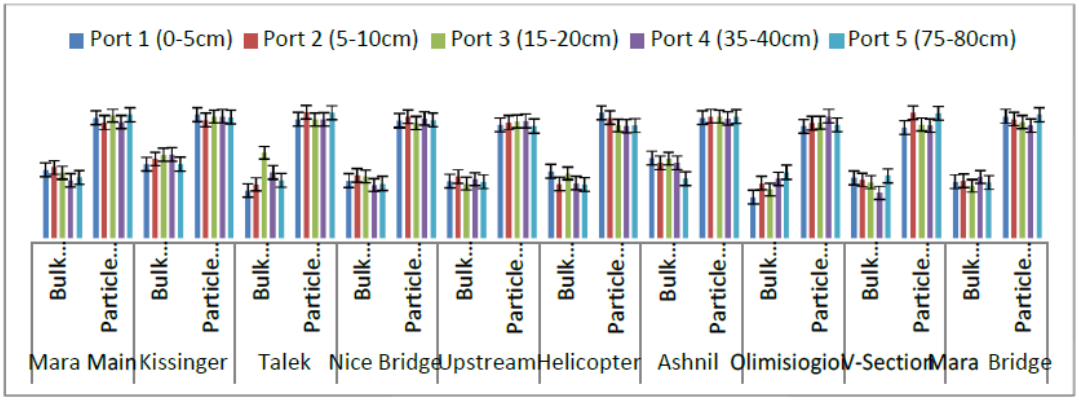

Fig. 6. General trend of bulk and particle densities in variation to soil depth across Maasai Mara rangeland ecosystem

Figure 6 indicates the variation of bulk and particle densities for MMNR selected representative sites in relation to soil depths from 0-5cm, 5-10cm, 15-20cm, 35-40cm, and 75-80cm. From the results, it can be noted that particle densities are higher than the bulk densities for most of the sites where sampling were done. At each stations elevation, five different depths or soil layers were used to determine both physical and hydraulic properties which shown the subsequent characteristics. The sand content ranged from 60% to 80%, clay from 14% to 30% and silt content from 6% to 10%. The particle density ranged from 2.3 gcm^{-3} to 2.7gcm^{-3} while the total porosity varied from 30.1 to 51% across the ecosystem. At 5-10 cm, MMNR main site was found to have a significantly lower bulk density of 2.37gcm^{-3} than P1, P3, P4, or P5 with bulk densities of 2.46, 2.50, 2.38, and 2.53 gcm^{-3}, respectively. At 75–80 cm, the particle density of this site was again significantly higher at 2.53gcm^{-3} as compared to other sites. Across MMNR rangeland ecosystem, it can be observed that no significant difference in particle density signifying homogenous total porosity across the ecosystem.

3.4 Total Organic Carbon

Table 3 shows that the total organic carbon (TOC) % decreases downward with soil depths and much of the concentration was found in the upper soil layer starting from 0-5cm, 5-10cm, 15-20cm, 35-40cm and 75-80cm respectively. As observed, Mara main site had the highest TOC concentration ranging from 2.25%, 2.00%, 1.49%, 1.13%, and 1.04% (Table 5). This was followed by Ashnil sites with 2.11%, 1.81%, 1.47%, 1.11%, and 0.42% with depth respectively. The soil samples collected at soil moisture, temperature sensor stations (5TM-ECH_2O) were analyzed by dry combustion following the Walkey and Black procedure [34]. Kissinger site has the least concentration of TOC ranging from the top soil surface content of 1.39% and the least 0.42% as compared to the other sites in the catchment. Table 6 shows an experimental site percentage concentration of total organic carbon, which indicates that top soil carbon concentration, is higher than bottom soil. The rangeland TOC concentration at the top soil layer was high as compared to the bottom layer, while most of the stations had more than 2.0% on upper layer while for the lower layer total organic carbon was less than 1.0%. The soil organic matter (SOM) was computed by multiplying the organic carbon concentration with Conventional Vanbameller factor of 1.724 following the method by [35]. This indicates that soil organic matter the MMNR rangeland ecosystem constitutes between 0.5% to approximately 4% by weight of the topsoil in upland soils. The average ideal soil consist of only 5% organic matter mainly composed of carbonaceous substances with soil biomass and remains of dead and living organisms.

According to [35], organic matter content of less than 1% is considerably low and are limited to desert areas while organic matter of more than 20% by weight are mainly peat soils which on low or high extremes reduce soil productivity. This finding of the soil characteristic at MMNR rangeland shows that it adversely suits the growth of grass vegetation with gradual topography, dominant flat surface, and homogeneous soils aggregated due to cyclic restorations of dead and living organisms caused by site decomposition of matter. The rangeland ecosystem consistently tends to increase in porosity and thus increases infiltration, aeration, percolation of water and their canopy cover reduces surface runoff and erosion hazards in wet season. The normal estimates of OM from loss-on-ignition (LOI) method are transformed to SOC usually assuming that 58% (1.724) of OM as composed by carbon [28]. Similar trend homogenously applied to all sites across the ecosystem.

In the analysis of variance, total organic carbon (TOC) had significant difference in concentrations with depth in various sites. The TOC and soil organic matter (SOM) concentration respectively decreased with increased depth from the soil surface across the ecosystem. The concentrations of both TOC and SOM were significantly high in Mara main site as compared to Kissinger and Ashnil sites, which had significantly low concentrations. However, the concentration at P1 (0-5cm) and P4 (35-40cm) had closely similar and higher concentrations as compared to other depths P2 (5-10cm), P3 (15-20cm), and P5 (75-80cm) in the three selected sites which acted as the representative samples. The Mean Square Error (MSE) was 1.675 indicating a more accurate concentration estimate percent for all sampled TOC from the ten-5TM-ECH_2O probe ecosystem sites. The sum of squares of all data values (SS) was 12.687; sum of squares of the all blocks (replicate) values was 14.523 and the sum of squares of all treatments (variety) was 0.103.

Mean Square of Profile (MSP) - 0.033. The least significant difference (LSD) between means at 5% level of probability (≤ 0.05) or 95% level of confidence was 4.473 and the F ratio was 0.072 with the degrees of freedom (df) of 49, mean square error (MSE) of 1.675 and sum of square error (SSE) of 0.745.

3.5 Maasai Mara National Reserve Rangeland Ecosystem Soil Chemical Properties

Soil laboratory analysis of MMNR ecosystem indicated that the potential of hydrogen (pH) ranged as 5.53 (medium acidic), 6.26 with slight acidity, 5.81 for medium acidic and 5.72 as medium acidic, segmented from top to bottom surface layer as 0-5cm, 10-15cm, 20-25cm and 25-30cm respectively. The other soil nutrients determined as suitable for grass and shrub growth were total nitrogen found respectively as 0.19%, 0.13%, 0.14%, and 0.18%, which were low in the soil. The total organic carbon was also present as 2.12%, 1.45%, 1.25%, and 2.07% and macro elements such as phosphorous measured in parts per million were found to be low in the soils with 5, 15, 5 and 10 ppm and potassium 1.04 me%, 0.48me%, 1.22 me% and 1.28me% which were also adequate. The amount of calcium, magnesium, manganese, copper, iron, and sodium were adequate in the soil layers while zinc were low in its concentration for soils in rangeland, which could have made rangelands suitable for grass mixed with sparse shrubs vegetation.

Table 3. Maasai Mara National Reserve sites total organic carbon concentration with soil depths

	Soil Depth (cm)				
Site TOC (%)	**Port 1 (0-5cm)**	**Port 2 (5-10cm)**	**Port 3 (15-20cm)**	**Port 4 (35-40cm)**	**Port 5 (75-80cm)**
Mara Main	2.25	2.00	1.49	1.26	1.04
Kissinger	2.39	1.95	1.58	1.32	0.82
Talek	2.28	1.84	1.75	1.16	0.98
Nice Bridge	2.29	1.98	1.72	0.92	0.46
Upstream	1.85	1.62	1.41	0.92	0.53
Helicopter	1.85	1.66	1.34	0.80	0.52
Ashnil	2.11	1.81	1.47	1.11	0.42
Olimisiogioi	2.30	2.13	1.86	1.20	0.64
V-Section	1.95	1.64	1.26	0.99	0.74
Mara Bridge	1.81	1.62	1.31	1.10	0.92
Sample Mean	2.11	1.83	1.52	1.08	0.71

Table 4. Sampled Ashnil site particle size distribution, total organic carbon, soil organic matter and texture class

Depth	**Sensor**	**pH (H_20)**	**Organic**	**%SOM**	**Mean Particle Size**			**Porosity**	**Hydraulic**	**Textural**
(cm)	**Horizon**		**Carbon (%TOC)**	**(%0C* 1.724)**	**Distribution**			**(%)**	**Conductivity (Ks)**	**Class**
					%Sand	**%Clay**	**%Silt**			
0-5	Port 1	5.53	2.11	3.64	68	23	9	40.5	40.18	SCL
5-10	Port 2	6.26	1.81	3.12	67	25	8	40.7	39.61	SCL
10-20	Port 3	5.81	1.47	2.53	58	35	8	42.0	30.51	SCL
35-40	Port 4	5.72	1.11	1.91	60	34	6	41.8	33.30	SCL
75-80	Port 5	5.86	0.42	0.72	59	34	8	41.8	31.41	SCL

Table 5: Statistical variation with depth of physical and chemical properties across Maasai Mara National Reserve rangeland ecosystem

Volumetric Water Content (m^3m^{-3})					
ANOVA	**Port 1 (0-5) cm**	**Port 2 (5-10) cm**	**Port 3 (15-20) cm**	**Port 4 (35-40) cm**	**Port 5 (75-80) cm**
Variance, V	0.001	0.003	0.004	0.008	0.005
Standard deviation, SD	0.025	0.056	0.062	0.087	0.067
Standard Error, SE	0.008	0.018	0.019	0.028	0.021
Coefficient of Variation, CV	0.166	0.257	0.239	0.295	0.206
Bulk Density (gcm^{-3})					
Variance, V	0.058	0.035	0.074	0.052	0.016
Standard deviation, SD	0.241	0.188	0.272	0.228	0.127
Standard Error, SE	0.076	0.059	0.086	0.016	0.040
Coefficient of Variation, CV	0.193	0.145	0.204	0.180	0.013
Particle Density (gcm^{-3})					
Variance, V	0.011	0.011	0.005	0.006	0.011
Standard deviation, SD	0.103	0.103	0.071	0.076	0.106
Standard Error, SE	0.032	0.032	0.022	0.024	0.034
Coefficient of Variation, CV	0.042	0.042	0.029	0.032	0.043
Total Organic Carbon Concentration (%)					
Variance, V	0.050	0.034	0.041	0.028	0.051
Standard deviation, SD	0.223	0.185	0.203	0.167	0.226
Standard Error, SE	0.070	0.059	0.064	0.053	0.071
Coefficient of Variation, CV	0.106	0.102	0.134	0.155	0.319

Table 5 shows the statistical variation with depth of important physical and chemical soil properties that influence soil moisture storage capacity. The volumetric water content variance ranged from minimal value of 0.001 to maximum value of 0.008, standard deviation from the mean ranged between 0.167 m^3m^{-3} and 0.226 m^3m^{-3}, standard error ranged between ±0.008, ±0.028, and coefficient of variation between 0.166 and 0.295 across the rangeland ecosystem. The bulk density also had its variance ranging from 0.016gcm^{-3} to 0.074gcm^{-3}, standard deviation between 0.127 gcm^{-3} and 0.272 gcm^{-3}, standard error ranged between ± 0.016 and ±0.068, and coefficient of variation ranged between 0.013 and 0.086 across the ecosystem. The other properties such as particle density varied between 0.005 and 0.011, standard deviation ranged between 0.071 and 0.106 gcm^{-3}, standard error ranged from ±0.022 to 0.034, with coefficient of variation from 0.029 to 0.043. The physical and chemical properties depicted significant difference with depth across the rangeland but the properties did not significantly affect soil moisture variation which shown homogenous characteristics on vegetation distribution.

From table 6, the analysis of variance indicates that the spatial mean soil moisture were significantly different throughout the profile with the surface top soil (0-5cm) being the lowest 0.153m^3/m^3 and the highest soil moisture content at lower depth (75-80cm) being 0.447m^3/m^3 respectively. This shows that volumetric water content increases with depth, a phenomenon that surface moisture is affected by environmental factors such as surface evaporation, rainfall runoff, soil infiltration, deep percolation and plant transpiration has direct influence on water storage and retention capacity within the soil matrix. Soil moisture variance ranged between 0.000 to 0.005, standard deviation and error ranged between 0.012 to 0.069 and ±0.005 to ±0.028 respectively. The standard deviation per soil moisture station was 0.104m3/m3. The coefficient of variation (CV) also ranged from 0.097 to 0.257 and the significant difference at ≤ 0.05 probability level was 0.428. The soil moisture significant differed from P1 to P5 (0-5cm) to (75-80cm) depth across all the moisture stations in the rangeland ecosystem. The sum of squares of all data values (SS) was 0.063; sum of squares of all blocks (replicate) values was 0.716 and the sum

Table 6. Analysis of variance (ANOVA) on spatial distribution of volumetric water content with depth at 10 m concentric distance to CRNS in Maasai Mara rangeland ecosystem (Main station)

Soil Depth (cm)	Volumetric water content (m^3m^{-3}) @ at 10m from CRNS footprint						Mean VWC (m^3m^{-3})	Variance	Standard deviation (m^3m^{-3})	Standard Error	Coefficient of variation
	0º-360º	60º	120º	180º	240º	300º	Spatial mean	V	SD	SE	CV
P1 (0-5) cm	0.14	0.16	0.16	0.17	0.14	0.15	0.153	0.000	0.012	±0.005	0.079
P2 (5-10) cm	0.17	0.18	0.22	0.25	0.18	0.28	0.213	0.002	0.045	±0.018	0.209
P3 (15-20) cm	0.19	0.27	0.36	0.36	0.27	0.33	0.297	0.004	0.066	±0.027	0.223
P4 (25-30) cm	0.25	0.39	0.43	0.41	0.30	0.36	0.357	0.005	0.069	±0.028	0.194
P5 (35-40) cm	0.30	0.42	0.47	0.47	0.38	0.39	0.405	0.004	0.064	±0.026	0.158
Mean	0.21	0.28	0.33	0.33	0.25	0.30	0.285	0.003	0.051	±0.021	0.173

Table 7. Analysis of variance on spatial distribution of volumetric water content with depth at 25 m concentric distance to CRNS in Maasai Mara rangeland ecosystem (main station)

Soil Depth (cm)	Volumetric water content (m^3m^{-3}) @ at 10m from CRNS footprint						Mean VWC (m^3m^{-3})	Variance	Standard deviation (m^3m^{-3})	Standard Error	Coefficient of variation
	0º-360º	60º	120º	180º	240º	300º	Spatial mean	V	SD	SE	CV
P1 (0-5) cm	0.13	0.16	0.17	0.16	0.15	0.14	0.152	0.000	0.015	±0.006	0.097
P2 (5-10) cm	0.18	0.19	0.17	0.23	0.19	0.24	0.200	0.001	0.028	±0.012	0.141
P3 (15-20)	0.20	0.26	0.39	0.37	0.29	0.36	0.292	0.006	0.075	±0.031	0.257

Soil Depth (cm)	Volumetric water content (m^3m^{-3}) @ at 10m from CRNS footprint						Mean VWC (m^3m^{-3})	Variance	Standard deviation (m^3m^{-3})	Standard Error	Coefficient of variation
	0º-360º	60º	120º	180º	240º	300º	Spatial mean	V	SD	SE	CV
cm											
P4 (25-30) cm	0.25	0.39	0.43	0.47	0.30	0.39	0.372	0.007	0.082	±0.034	0.221
P5 (35-40) cm	0.29	0.45	0.46	0.50	0.36	0.37	0.405	0.006	0.078	±0.032	0.193
Mean	0.21	0.29	0.32	0.35	0.26	0.30	0.284	0.004	0.056	±0.023	0.182

Table 8. Spatial distribution of volumetric water content with depth at 75 m concentric distance to CRNS in Maasai Mara rangeland ecosystem (Main station)

Soil Depth (cm)	Volumetric water content (m^3m^{-3}) @ at 10m from CRNS footprint						Mean VWC (m^3m^{-3})	Variance	Standard deviation (m^3m^{-3})	Standard Error	Coefficient of variation
	0º-360º	60º	120º	180º	240º	300º	Spatial mean	V	SD	SE	CV
P1 (0-5) cm	0.15	0.16	0.16	0.17	0.14	0.16	0.157	0.000	0.010	±0.004	0.066
P2 (5-10) cm	0.18	0.19	0.18	0.23	0.18	0.24	0.200	0.001	0.028	±0.011	0.138
P3 (15-20) cm	0.19	0.23	0.33	0.39	0.27	0.34	0.292	0.006	0.075	±0.031	0.257
P4 (25-30) cm	0.19	0.39	0.42	0.49	0.30	0.38	0.362	0.011	0.104	±0.043	0.288
P5 (35-40) cm	0.33	0.42	0.46	0.51	0.37	0.36	0.408	0.005	0.068	±0.028	0.166
Mean	0.21	0.28	0.31	0.36	0.25	0.30	0.280	0.046	0.057	±0.023	0.183

Table 9. Analysis of variance on spatial distribution of volumetric water content with depth at 175 m concentric distance to CRNS in Maasai Mara rangeland ecosystem (Main station)

Soil Depth (cm)	Volumetric water content (m^3m^{-3}) @ at 10m from CRNS footprint						Mean VWC (m^3m^{-3})	Variance	Standard deviation (m^3m^{-3})	Standard Error	Coefficient of variation
	0º-360º	60º	120º	180º	240º	300º	Spatial mean	V	SD	SE	CV
P1 (0-5) cm	0.17	0.14	0.16	0.16	0.14	0.16	0.166	0.000	0.0122	±0.0050	0.0790
P2 (5-10) cm	0.17	0.19	0.18	0.25	0.16	0.26	0.202	0.002	0.0426	±0.0174	0.2114
P3 (15-20) cm	0.17	0.22	0.36	0.39	0.29	0.35	0.297	0.008	0.0866	±0.0354	0.2920
P4 (25-30) cm	0.19	0.40	0.39	0.56	0.27	0.38	0.365	0.016	0.1263	±0.0516	0.3460
P5 (35-40) cm	0.27	0.44	0.45	0.59	0.34	0.36	0.408	0.012	0.1113	±0.0454	0.2724
Mean	0.19	0.28	0.31	0.39	0.24	0.30	0.288	0.008	0.076	±0.0310	0.2402

Table 10. Analysis of variance on volumetric water content as per 5TM-ECH$_2$0 Probes

Soil Depth (cm)	Weighted average 5TM-ECH$_2$O VWC (m^3m^{-3}) spatially distributed sites										Mean VWC (m^3m^{-3})	Standard deviation (m^3m^{-3})	Standard Error	Coefficient of variation
	Mara Main	Kissinger	Talek	Nice Bridge	Upstream	Helicopter	Ashnil	Olimisiogioi	V-Section	Mara Bridge	Spatial mean	SD	SE	CV
P1 (0-5) cm	0.14	0.15	0.17	0.14	0.11	0.13	0.13	0.15	0.16	0.20	0.147	0.0249	±0.00249	0.1679
P2 (5-10) cm	0.21	0.19	0.15	0.24	0.14	0.16	0.30	0.28	0.23	0.26	0.216	0.0511	±0.01615	0.2365

Soil Depth (cm)	Weighted average 5TM-ECH_2O VWC (m^3m^{-3}) spatially distributed sites										Mean VWC (m^3m^{-3})	Standard deviation (m^3m^{-3})	Standard Error	Coefficient of variation
	Mara Main	Kissinger	Talek	Nice Bridge	Upstream	Helicopter	Ashnil	Olimisiogioi	V-Section	Mara Bridge	Spatial mean	SD	SE	CV
P3 (15-20) cm	0.21	0.29	0.14	0.26	0.19	0.24	0.31	0.31	0.32	0.31	0.258	0.0616	±0.01948	0.2388
P4 (25-30) cm	0.28	0.29	0.18	0.31	0.30	0.18	0.25	0.43	0.29	0.44	0.295	0.0838	±0.02651	0.2841
P5 (35-40) cm	0.27	0.40	0.23	0.29	0.32	0.32	0.30	0.45	0.29	0.39	0.326	0.0000	±0.00000	0.0000
Mean	0.22	0.26	0.17	0.25	0.21	0.21	0.26	0.32	0.26	0.32	0.248	0.0443	±0.0129	0.1855

of squares of all treatments (variety) was 0.103. Mean Square of Profile (MSP) - 0.077. The least significant difference (LSD) between means at 5% level of probability (≤ 0.05) or 95% level of confidence was 0.428 and the F ratio was 7.135 with the degrees of freedom (df) of 35, mean square error (MSE) of 0.0108 and sum of square error (SSE) of 0.2688.

From tables 7, 8 and 9, it can be noted that the volumetric water content with respect to depth on spatial scale (10, 25, 75, and 175 m) distance varied increasingly at near surface 0-5cm shallow depth to deep 75-80cm depth. The mean concentric VWC ranged from 0.152 m^3m^{-3} to 0.284 m^3m^{-3} and their variance ranged between 0.000 and 0.005, standard deviation between 0.0443 m^3m^{-3} and 0.057 m^3m^{-3}, standard error between ±0.0129 and ±0.0310 and coefficient of variation ranged between 0.173 and 0.240 as the concentric distance increases. The distribution of soil moisture with depth is a function of environmental influence caused by evaporation at near the soil surface, infiltration, runoff and percolation including the immediate soil conditions and surface vegetation cover which determines rooting depth of plants. The deeper the roots of vegetation the farther the soil moisture storage from the soil surface, plants roots response positively towards water available soil matrix and elongates as much as possible depending on extractable water content in the soil. In this rangeland ecosystem, the maximum rooting depth was observed to be approximately 30cm to 40cm for grass of nearly the same species. The grass roots were dense at near the soil surface as compared to the bottom- layered soil.

Table 10 indicates spatial variation of VWC and its mean ranging between 0.147m^3m^{-3} at the top soil profile (0-5cm) and 0.326m^3m^{-3} at below the soil depth of 75-80cm respectively. The soil moisture content decreased with depth. The standard deviation increased from the top layer to the bottom soil layer ranged from 0.0249 to 0.0838m^3m^{-3} and the standard error ranged from ± 0.0000 to ±0.02651 while the coefficient of variation ranged from 0.0000 to 0.2841. The table shows that P1 (0-5cm) profile has significantly less moisture as compared to spatial means of all stations depths for P5(75-80cm) except at Kissinger which has no significantly different soil moisture at depth P3 and P4 (15-20, 35-40cm). In addition, at Talek site, the soil moisture was significantly less at all depths and more as compared to Olimisiogioi location except at Kissinger location. The sum of squares of all data values (SS) was 0.371; sum of squares of the all blocks (replicate) values was 0.194 and the sum of squares of all treatments (variety) was 0.103. The least significant difference (LSD) between means at 5% level of probability (≤0.05) or 95% level of confidence was 0.624 and the F ratio was 0.352 with the degrees of freedom (df) of 49, mean square error (MSE) of 0.033 and sum of square error (SSE) of 0.073.

Table 10 and figure 7 illustrate the effect of sample size on the standard error in soil moisture estimates calculated for (10) 5TM-ECH_20 and CRNS network. Standard errors have been calculated for the driest and wettest calibration sets at each site of concentric distance of CRNS. For all sites, the vast majority of the reduction in sample standard error occurred within the sampling sites, which were taken to be the predicted representation of the entire ecosystem and empirical standard across the CRNS and 5TM-ECH_20 network. Soil moisture variability increase more rapidly below the soil surface and the vice versa is true within profile levels and sites, there was a general trend where less variability occurred during dry conditions as compared to wet conditions.

3.6 Time Series Analysis of Volumetric Water Content in Maasai Mara Ecosystem

Fig. 8 shows the time series variation of VWC in relation to rainfall events, which occurred in 2017 and Mid-April 2018, it can be noted that rainfall was high in the month of April and May 2018 with depicting rainfall range of 0.89 to 3.91 mm with VWC ranging from 0.40 m^3m^{-3} to 0.436 m^3m^{-3}. During the period of prolonged dryness or no rains or little rains (blue lines), fraction of soil moisture remains in the soil (red lines) and this was depicted during the previous year in periods in 2017 and 2018 with rainfall range between 0, 0.59 to 1.29 with VWC range between 0.25 to 0.38 m^3m^{-3}. This indicates that soil moisture retention in soil enables rangeland vegetation survive under stored moisture during seasons of no rainfall for a certain period before wilting threshold is reached and complete drying. A time series of the CRNS soil moisture data shows the dependency of the soil moisture fluctuations on rainfall.

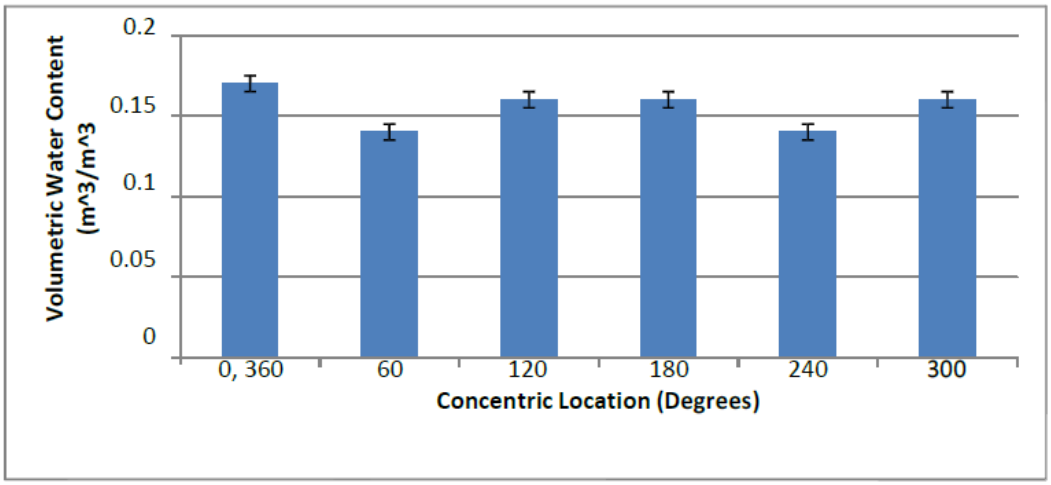

Fig. 7. Variation of gravimetric water content at 0-5cm soil depth within the CRNS

Fig. 9 indicates high volumetric water content occurrence with low temperature condition inversely proportional resulting in the variation of soil moisture storage and retention capacity. The relationship between the two environmental factors shows that for soil moisture to be stored for long period after a rainfall event, low temperature, infiltration rate, rainfall runoffs, and deep percolation must coexist within the soil and this relies greatly on soil texture and structure. This gradual declined can be explained due to massive soil water loss through evaporation as during this time, crop cover had not fully covered the soil to reduce soil evaporation. Soil water percolates through soil profile only when proceeded soil is satisfied i.e. has reached its field capacity, above which excess water is left free to percolates down the soil profile. This finding corroborate with an experiment of water application in an irrigation scheme by [36] found that before water arriving in last layer, it had to satisfy the above-lying soil profiles. This observation is similar to that of many literatures, which explain that fluctuations of soil water contents in bottom layers of soil profiles are small compared to top layer.

Fig. 10 shows similar behavior in soil water and temperature relations, which indicates an inverse proportional characteristic in that during the month of September through December 2017, there was low moisture due to high temperature and oscillating variation of soil moisture with temperature. Low moisture content was also experience at near surface layer VWC1 (0-5cm) and high below soil surface oscillating between VWC4 (35-40cm) and VWC5 (75-80cm) layer respectively. It was also observed that the trend of volumetric water content spatially distributed across the ecosystem with depth shows top soil layer P1 (0-5cm) has significantly low moisture content as compared to deep shallow layers P4 (35-40cm) and P5 (75-80cm). This was supported by findings that soil moisture at this shallow depth was often intensively affected by plant root systems [37, 38]. In addition, semi-arid regions, more soil moisture evaporation caused by high temperature usually occur on upper positions as they suffer more solar radiation and wind that affect plant growth. This indicates low moisture near the soil surface and high moisture content below the soil surface with low environmental influence on soil moisture storage across the ecosystem.

Table 11 shows the average bulk density, ω_{lat} and $wSOM$ for each point in degrees of the main Mara site where CRNS values were collected. The dry soil bulk density varied from 1.19 g cm^{-3} to 1.45g cm^{-3}. In the computation of volumetric soil moisture, the bulk density was used to convert gravimetric soil moisture content and determine the effective depth to which the CRNS probes measured the soil moisture at a given point ranged from 11 and 12cm. The sites had varied lattice water (water of crystallization) of 0.02gg^{-1} at its lowest and 0.03gg-1 at the highest, which may be assumed negligible. Sandy Clay loam (SCL) majorly the top soil has the highest $SOM\ water$ as compared to the bottom sandy clay soil. The content varied from 0.002 to 0.03 gg−1. The range of average values was between 673.48 to 899.94 counts per hour (ch^{-1}) with coefficients of variation during the dry

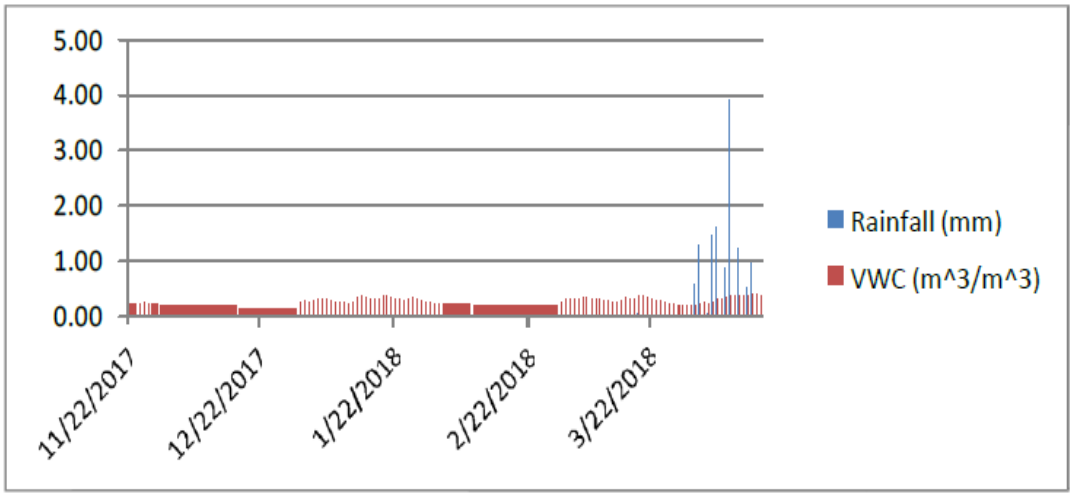

Fig. 8. Time series rainfall correlation to volumetric water content between Nov 2017-April 2018

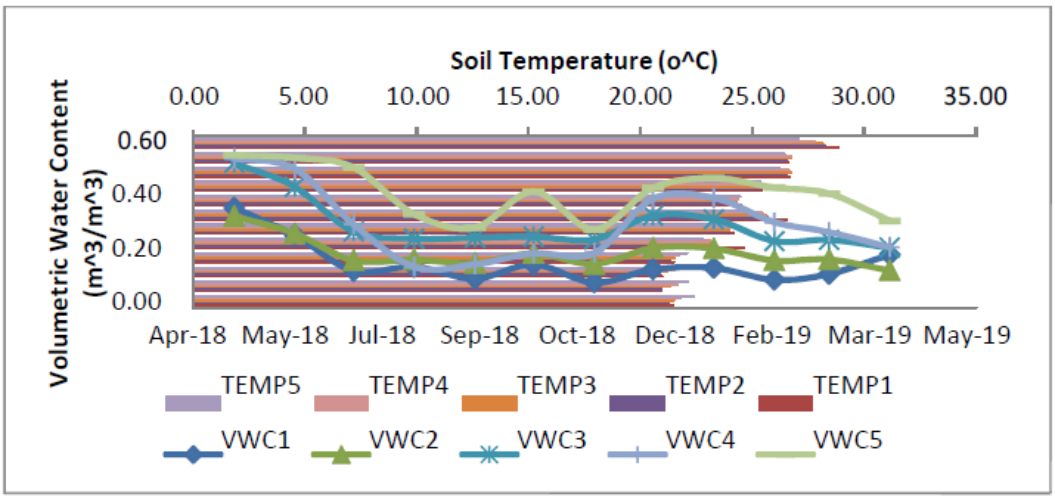

Fig. 9. Trend of monthly soil moisture and temperature variation per depths at Kissinger 5TM-ECH$_2$O site: 2018-2019

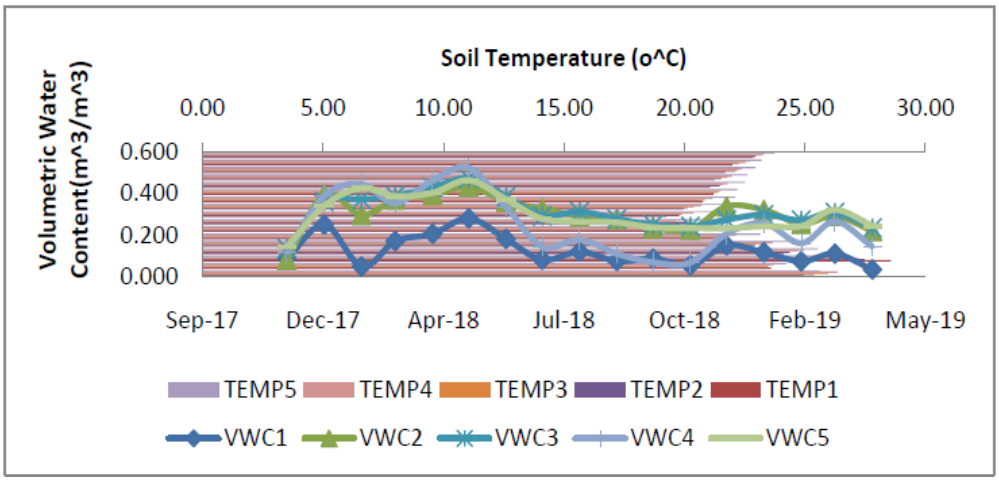

Fig. 10. Variation of Ashnil site soil moisture and temperature at different soil profiles

Table 11. Cosmic ray volumetric water content according to soil layers at Mara Main station

Soil Depth (cm)	$N_{corr}(ch^{-1})$	$N_o(ch^{-1})$	$\rho_{bd}(gcm^{-3})$	$\omega_{lattice}(gg^{-1})$	$SOM_{water}(gg^{-1})$	Average Volumetric water content (m^3m^{-3})	Effective depth (cm)
0-5	565	1441	1.40	0.03	3.64	0.34	11
5-10	565	1430	1.45	0.03	3.12	0.35	11
10-15	565	1414	1.34	0.03	2.53	0.32	11
15-20	565	1388	1.19	0.03	1.91	0.29	12
20-25	565	1363	1.25	0.03	1.52	0.30	12
25-30	565	1269	1.22	0.03	0.72	0.29	12

N_{corr} – Corrected neutrons, N_O – Average neutron intensity, ρ_{bd} - Dry bulk density, $\omega_{lattice}$ - Lattice water, SOM water - Soil organic matter expressed as water equivalent

season and 241.12 to 114.71 ch^{-1} during the wet season, for sites with its average measurement depths (*z**) ranged between 0 and 30 cm where the soil moisture was a reciprocal to the depths. The effective measurement depth of CRNS over the 1-year period between Dec 2017 and April 2018 (Table 11) showed that the effective measurement depth ranged from 10.58 cm to 12.48cm,with an average effective measurement depth scale of 11.53cm. The minimum and maximum depths of measurement were 5cm to 80cm with soil moisture ranged from as high as 0.35m^3m^{-3} to 0.29m^3m^{-3} respectively and to 0 m^3m^{-3} for dry soils at the bottom layer of 80cm across the concentric distance. This shows that between 10m to 175m away from the CRNS footprint, fraction of soil moisture exist where general cover is of dominant grassland and it signifies that grassland soil does not reach complete dryness between the bi-seasons.

3.6.1 Converting Neutron Counts to Soil Moisture

In the study, the conversion of the neutron count rate to gravimetric soil water equivalent θ_{grv} was performed according to [24] who suggested a theoretical relation that has been applied successfully by the majority of CRNS studies. Figure 11 illustrates the time series of daily rainfall and moderated neutron counts at the study site for the period 2017 and 2018. It can be observed that the corrected moderated counts decrease sharply with precipitation and increase slowly following an exponential shape caused by fluctuating rainfall. Once a rainfall event occurs, moisture in the footprint increase immediately, thus, neutron intensity decreases fast and the calculated CRNS soil moisture increases rapidly since it is inversely proportional because of

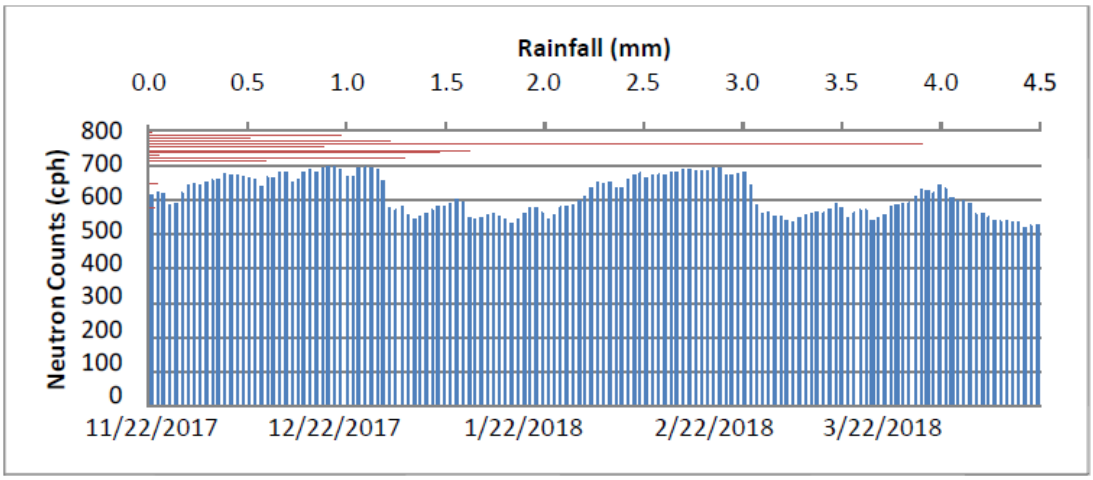

Fig. 11. Time series of daily rainfall and moderated neutron counts during the period 2017 and 2018 at Maasai Mara National Reserve

moderation effect caused to neutrons by hydrogen atoms. The CRNS exhibiting have shorter response times and greater apparent soil moisture. Different rainfall levels also have different characteristics, thus soil moisture increases in trend with increased rainfall while on the other hand when soil is drying out, derived CRNS soil moisture declines gradually. This corroborated with findings of [39] who found that spatial correlation length varied as a function of soil moisture content. This however, various controls may lead to a deviation of normal behavior and may increase or decrease soil moisture variance [40, 41]. At a grassland site, an increase in correlation scale was found with increasing wetness whereas no increase in correlation scales in a forest site. The table indicates the hourly VWC determined using the calculated N_o value in the rearranged calibration function equation (2.10).

3.6.2 Biomass Water Equivalent

Simultaneous measurements of area-averaged soil water content and neutron count in calibration were required and site-specific calibrations implicitly included vegetation effects on the observed neutron counts (Table 12). MMNR rangeland ecosystem being dominant natural grassland, the experimental sites had no significant variations of biomass (grassland), the biomass correction was therefore not required, as the change in hydrogen of the biomass within the site was 1.34mm of H_2O, and this value was insignificantly small and was ignored in the calibration. This was in similarity with [42] who demonstrated an approach to isolate the effect of vegetation on the neutron intensity signal and estimated area average biomass water equivalent in agreement with independent measurements. [7] also found a linear relationship based on measurements for maize (Zea mays L.) and soybean [Glycine max (L.) Merr.], finding was that a 1% decrease in N0 for every 1 kg/m^2 of biomass or water equivalent present.

Here, biomass water equivalent decreased with corresponding increased neutron counts.

3.6.3 Root Biomass Density

Five cored soil samples were collected from MMNR sites with homogenous characteristics across rangeland via a core ring of volume 98.175cm3 (0.098175lts) at different soil layers of 0-5, 5-10, 15-20, 35-40 and 75-80 cm and during the lab measurements their ambient/room temperature was taken to be 24oC. The samples were used to determine the root density of the soil and that the densities decreased with increased depth. The root density at the top soil layer of 0-5cm was higher with 8.098g/l as compared to the density at the bottom layer of 75-80cm with 0.682g/l. The fine root distribution decreased with soil depth and decreased with distance from the plant stem in sandy clay loam soil. The observed grass height within the rangeland ranged between 80cm and 120cm tall. The plant extracts water preferentially according to the length of roots per unit soil volume. Usually the greatest root density is in a few centimeters below the surface soil that dries first due to heat exposure resulting into evaporation of moisture. The volumetric water content was obtained by direct sampling of known soil volume within the periphery of installed CRNS and 5TM-ECH$_2$O probes that were used to estimate, θ_v.

The storage capacity of soil moisture in the plant root zone highly depends on the amount of soil textural classes, rainwater, fractional amount that infiltrates into the soil and that which percolates into and partly that goes as runoff. The spatial variation of mean soil moisture were significantly different with depth across rangeland since the top soil layer (0-5cm) had the lowest 0.11m^{3}m^{-3} and the highest soil moisture content at the deepest layer (75-80cm) with 0.45m^{3}m^{-3} (Figure 12). The mean volumetric water content at spatially distributed sites with depth of 5cm was mainly 0.13m^{3}m^{-3} for most of the 5TM-ECH$_2$O stations with textural class of sandy clay loam soil. The stations with sandy clay soils however had volumetric water content of 0.11m^{3}m^{-3} with an exception of olimisigioi site where the water content was 0.14m^{3}m^{-3} and the surrounding environment dominated by grassland mixed with sparse shrubs. The standard mean deviation of the available water to plants was 0.011m^{3}m^{-3} and its standard error was ± 0.003. A study by [43] showed that the standard deviation of soil moisture peaked between 0.17cm^{3}cm^{-3} and 0.23cm^{3}cm^{-3} for most textural classes. The magnitude of soil moisture variability was controlled by the interplay of soil hydraulic properties and climate. The average moisture at which the maximum variability occurred depended on soil hydraulic properties and vegetation.

Table 12. Calibrations, dates, gravimetric soil moisture, bulk density, neutron counts and calculated N_o values

Calibration date	Moisture status	Gravimetric water content (gg^{-1})	Bulk Density (gcm^{-3})	Volumetric Water Content(m^3m^{-3})	Neutron Count (ch^{-1})	No
12/12/2017	Dry	0.129	1.40	0.180	665.747	1647.187
21/12/2017	Dry	0.097	1.45	0.140	697.625	1724.343
05/04/2018	Wet	0.219	1.19	0.260	589.417	1462.438
09/04/2018	Wet	0.295	1.22	0.360	540.708	1344.558
Mean						*1544.631

**Calculated average No value for calibration was 1544.631*

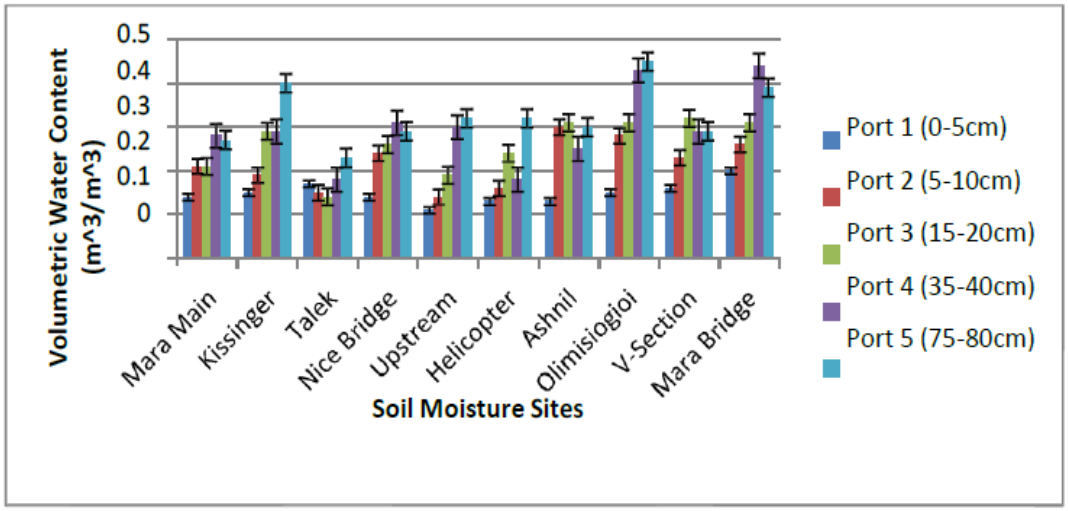

Fig. 12. Spatial distribution of weighted average volumetric water content with depth across Maasai Mara rangeland

Table 13. Statistical indicators comparing performance of the three approaches applied to describe the measured soil water content across MMNR rangeland ecosystem

Method/Technique	NSE	r	RMSE	R^2
Cosmic Ray Neutron Sensor (CRNS) probe	0.779	0.000	0.0111	0.779
5TM-ECH$_2$0 probes	0.978	0.000	0.0332	0.993
Gravimetric Water Content	0.998	0.000	0.0035	0.998
Overall Performance	0.918	0.000	0.0159	0.923

Table 13 shows the statistical performance of three soil water content determination approaches and through their mean comparisons, gravimetric water content gave significantly higher performance with Nash Sutcliffe Efficiency (NSE) of 0.998, r = 0.000, RMSE = 0.0035 and the coefficient of correlations, R^2 was 0.998. The 5TM-ECH$_2$0 approach gave fairly predicted as compared to cosmic ray neutron sensor technique with NSE = 0.978, r = 0.000, RMSE = 0.0332 and R^2 = 0.933 in relation to the overall model performance prediction results of NSE = 0.918, r = 0.000, RMSE = 0.0159 and R^2 = 0.923.

3.4 Statistical Analysis

Analysis of variance (ANOVA) for randomized complete block design (RCBD) was applied to compare the influence of soil moisture variability with depth on soil physical properties of the ten-(10) 5TM-ECH$_2$0 sites. Significantly, different means were separated using least significant difference (LSD) at 5% level of probability ($P \leq 0.05$).

4. CONCLUSION

In this study, soil moisture content was normally

distributed with depth and in the horizontal plane throughout the rangeland depending on oscillating annual precipitation. Based on soil moisture depths observation at various sites, relatively lower soil moisture content across the rangeland ecosystem was present in the top soil layers. The analysis of MMNR rangeland ecosystem soil shown that, there was no significant difference in mean bulk density, particle density, and textural classes across sites with depths to soil moisture variation. Total organic carbon had no significant effect on soil moisture storage at near

the soil surface since the concentration of TOC was high near the surface and decreased gradually down the soil surface. This resulted in significant differences in soil moisture within depth increments where the variation in moisture was low near the surface. Soil moisture storage was generally expressed as volumetric water content per unit area measured to a specific depth. The presence of varied vegetation covers but majorly dominated by grassland is because of shallow soil moisture hence low effective rooting depth; however, semi-arid scenarios are prone to short vegetation cover. These zones are characterized by high vegetation transpiration and soil evaporation caused by temperature variation with presence of relatively higher stable moisture values in deeper layers. In overall comparison, the derived CRNS soil moisture followed the general trend of the in-situ variation of soil moisture despite its underestimation; however the soil moisture levels across the rangeland ecosystem may reasonably sustain grassland vegetation for increasing wildlife carrying capacity.

COMPETING INTERESTS

Authors have declared that no competing interests exist.

REFERENCES

1. Stewart JB, Engman ET, Feddes RA, Kerr Y, editors. Scaling up in hydrology using remote sensing. Chichester: Wiley. 1996;255.
2. Figueiredo de T, Royer AC, Fonseca F, de Araújo Schütz FC, Hernández Z. Regression Models for Soil Water Storage Estimation Using the ESA CCI Satellite Soil Moisture Product: A Case Study in Northeast Portugal. Water. 2021;13:37. Available:https://doi.org/10.3390/w13010037
3. Pierini NA, Vivoni ER, Robles-Morua A, Scott RL, Nearing MA. Using observations and a distributed hydrologic model to explore runoff thresholds linked with mesquite encroachment in the Sonoran Desert. Water Resource Research. 2014;50:8191–8215.
4. Templeton RC, Vivoni ER, Méndez-Barroso LA, Pierini NA, Anderson CA, Rango A, Laliberte AS, Scott RL. High-resolution characterization of a semiarid watershed: Implications on evapotranspiration estimates, Journal of Hydrology. 2014; 509, 306–319.
5. Franz T, Wang T, Avery W, Finkenbiner C, Brocca L. Spatiotemporal characterization of soil moisture fields in agricultural areas using cosmic-ray neutron probes and data fusion. EGU General Assembly. Vienna, Austria. 2015;12–17.
6. Bullied WJ, Entz MH. Soil water dynamics after alfalfa as influenced by crop termination technique. Agronomy Journal. 1991;91:294–305.
7. Western AW, Grayson RB, Bloschl G, Willgoose G, McMahon TA. Observed spatial organization of soil moisture and relation to terrain indices, Water Resource Research. 1999;35(3):797–810.
8. Bell JE, Sherry R, Luo Y. Changes in soil water dynamics due to variation in precipitation and temperature: An eco-hydrological analysis in a tallgrass prairie, Water Resources Research. 2010;46:W03523. DOI:10.1029/2009WR007908.
9. Hudson JA. The contribution of soil moisture storage to the water balances of upland forested and grassland catchments, Hydrological Sciences Journal, 1988;33:3:289-309. DOI:10.1080/02626668809491249.
10. Prince, Khaldoun Rishmawi, Stephen D. and Yongkang Xue. Vegetation Responses to Climate Variability in the Northern Arid to Sub-Humid Zones of Sub-Saharan Africa; 2016.
11. Gerten D, Schaphoff S, Lucht W. Potential future changes in water limitations of the terrestrial biosphere, Climate Change. 2007;80:277–299. DOI:10.1007/s10584-006-9104-8.
12. Olson RJ, Johnson KR, Zheng DL, Scurlock JMO. Global and Regional Ecosystem Modeling: Databases of Model

Drivers and Validation Measurements. ORNL Technical Memorandum TM-2001/196.Oak Ridge National Laboratory, Oak Ridge, Tennessee; 2000.
13. Karkanis P, Au K, Schaalje G. Comparison of four measurement schedules for determination of soil particle-size distribution by the hydrometer method. Can Agricultural Engineering. 1991;33:211–216.
14. Saxton KE, Rawls WI, Romberger lS, Papendick RI. Estimating generalized soil-water characteristics from texture. Soil Science Society of America Journal. 1986;50:1031-1036. Blake GR, Hartge KH. Bulk Density. Methods of Soil Analysis, Part 1, American society of soil
15. Science Journal, Madison, WI, USA. 1986;363-376.
16. Soil Survey Staff. Keys to soil taxonomy, 12th edition. USDA Natural Resources Conservation Service; 2014.
17. Nelson DW, Sommers LE. Total carbon, organic carbon, and organic matter. In: Sparks, D.L., editors, Methods of Soil Analysis. SSSA Book Ser. 5. SSSA, Madison. 1996;961–1010.
18. Thompson SE, Harman CJ, Heine P, Katul GG. Vegetation-infiltration relationships across climatic and soil type gradients, Journal of Geophysical Research, 2010;115:G02023/ DOI:10.1029/2009JG001134.
19. Zhang Y, Carey SK, Quinton WL, Janowicz JR, Pomeroy JW, Flerchinger GN. Comparison of algorithms and parameterizations for infiltration into organic-covered permafrost soils, Hydrology Earth System Science. 2010;14:729–750, DOI:10.5194/hess- 14-729-2010.
20. Ayu IW. Assessment of infiltration rate under different dry land types in Illerlive Sub district, Sumbuwa Bester. Indonesia. Journal of Natural Science Research. 2013;3(10):71-76.
21. Koorevaar P, Menelik G, Dirksen C. Elements of soil physics. Elsevier Science, Amsterdam; 1983.
22. Bouwer H. Intake rate: Cylinder infiltrometer. In A. Klute (ed.) Methods of soil analysis. Part 1. 2nd ed. SSSA Book Ser. 5. SSSA, Madison, WI; 1986; 825–844.
23. Zreda M, Desilets D, Ferre TPA, Scott RL. Measuring soil moisture content non-invasively at intermediate spatial scale using cosmic-ray neutrons. Geophysical Research Letters. 2008;35, L21402:1–L21402:5.
24. Desilets D, Zreda M, Ferre TPA. Nature's neutron probe: Land surface hydrology at elusive scale with cosmic rays, Water Resource Research, 2010;46, W11505,. DOI:10.1029/2009WR008726.
25. Zreda M, Shuttleworth WJ, Zeng X, Zweck C, Desilets D, Franz T, Ferre TPA. COSMOS: The Cosmic-ray Soil Moisture Observing System. Hydrology of Earth System Science, 2012;16:4079- 4099.
26. Franz TE, Zreda M, Ferré TPA, Rosolem R, Zweck C, Stillman S, Zeng X, Shuttleworth WJ. Measurement depth of the cosmic ray soil moisture probe affected by hydrogen from various sources, Water Resources Research. 2012b;48:W08515. DOI:10.1029/2012WR011871
27. Ball DF. Loss-on-ignition as an estimate of organic matter and organic carbon in non-calcareoussoils. Journal of Soil Science. 1964;15:84–92
28. Davies BE. Loss-on-ignition as an estimate of soil organic matter. Proceedings of Soil Science Society of America 1974;38:150–151
29. Hawdon A, McJannet D, Wallace J. Calibration and correction procedures for cosmic-ray neutron soil moisture probes located across Australia, Water Resource. Research. 2014;50:5029–5043. DOI: 10.1002/2013WR015138.
30. Bogena HR, Huisman JA, Baatz R, Franssen HJH, Vereecken H. Accuracy of the cosmic- ray soil water content probe in humid forest ecosystems: The worst-case scenario. Water Resource Research. 2013;49:5778–5791. DOI:10.1002/wrcr.20463.
31. Franz T. Stationary probe data calculations. Lincoln, NE: Franz Hydro-geophysics Lab Group, University of Lincoln-Nebraska. 2014;1-4;.
32. SAS. Statistical Analysis Systems Institute. Version 9.1, SAS Institute Inc., Cary, North Carolina, USA; 2008.
33. Van Engelen VWP, Dijkshoorn JA. Global and National Soils and Terrain Digital Database (SOTER). Procedures Manual Version 2.0, ISRIC - World Soil Information, Wageningen: ISRIC; 2013.
34. elson DW, Sommers LE. Total carbon, organic carbon, and organic matter. In: Sparks, D.L., editors, Methods of Soil Analysis. SSSA Book Ser. 5. SSSA,

Madison. 1996;961–1010.
35. Howard PJA, Howard DM. Use of organic carbon and loss-on-ignition to estimate soil organic matter in different soil types and horizons. Biology and Fertility of Soils. 1990;9:306–310.Available:https://doi.org/10.1007/BF00634106
36. John Mthandi, Fredrick C, Kahimba, Andrew KPR. Tarimo Baandah A. Salim,Max W. Lowole. Modification, Calibration and Validation of APSIM to Suit Maize (Zeamays L.) Production System: A Case of Nkango Irrigation Scheme in Malawi. American Journal of Agriculture and Forestry. Special Issue: Agriculture Ecosystem and Environment. 2014; 2(6-1):1-11. DOI:10.11648/j.ajaf.s.2014020601.11
37. Cong X, Liang Y, Li D. Root characteristics of Hippophae rhamnoides and dynamic of soil water in semi-arid on Loess Plateau, Bull. Soil Water Conservation. 1990;10:98–103.
38. February EC, Higgins SI. The distribution of tree and grass roots in savannas in relation to soil nitrogen and water, South African Journal of Botany. 2010;76:517–523.
39. Zehe E, Graeff T, Morgner M, Bauer A, Bronstert A. Plot and field scale soil moisture dynamics and subsurface wetness control on runoff generation in a headwater in the Ore Mountains. Hydrology of Earth System Science. 2010;14 (6):873–889
40. Das NN, Mohanty BP, Cosh MH, Jackson TJ. Modeling and assimilation of root zone soil moisture using remote sensing observations in Walnut Gulch Watershed during SMEX04. Remote Sensing of Environment. 2008;112(2):415–429.
41. Wu X, Liu M, Wu Y. In-situ soil moisture sensing: optimal sensor placement and field estimation. ACM Transition of Sensing Networks, Environmental journal of Earth Science. 2012;63(3):477-488.
42. Franz TE, Zreda M, Rosolem R, Hornbuckle BK, Irvin SL, Adams H, Kolb TE, Zweck C, Shuttleworth WJ. Ecosystem-scale measurements of biomass water using cosmic ray neutrons, Geophysical Research Letters. 2013a 40:3929–3933. DOI:10.1002/grl.50791.
43. Vereecken HT, Kamai T, Harter R, Kasteel J, Hopmans J. Vanderborght. Explaining soil moisture variability as a function of mean soil moisture: A stochastic unsaturated flow perspective, Geophysical Research Letters. 2007;34:L22402. DOI:10.1029/2007GL031813.

Peer-review history:
The peer review history for this paper can be accessed here:
https://www.sdiarticle4.com/review-history/72533